

## STFC ISIS Neutron and Muon Source

## Monte Carlo Comparison of ESS LoKI Day 1 with SANS2D at ISIS

### Team

Robert M Dalgliesh robert.dalgliesh@stfc.ac.uk

September 2025

# Table of Contents

1	Introduction	2
2	Instrument Layout    2.1 SANS2D     2.2 LoKI	2 3
3	MonteCarlo Simulations    3.1 Intensity Normalisation     3.1.1 SANS2D     3.1.2 LoKI	4
4	Simulation Results	4
5	Conclusions	7
6	Acknowledgements	ę

#### 1 Introduction

The LoKI instrument [1] is located at the European Spallation Source (ESS) in Lund, Sweden. It has been designed, manufactured and constructed by ISIS based on the instrument concept developed by ESS and has recently been delivered and installed at the ESS. LoKI intended to function as a broad bandwidth small angle scattering (SANS) instrument delivering a wide range of science over a large simultaneous q range. It will be complemented by SKADI [2], a second broad bandwidth that has been developed by FZ-Julich and LLB that will include neutron polarisation capabilities for magnetism studies. In this document the simulated, predicted day one performance of LoKI will be compared to that of the simulated performance of SANS2D at ISIS. SANS2D is also a broad bandwidth, multi-purpose SANS instrument located on the ISIS Second Target Station (TS2) it has been in operation since 2009. The instrument delivers exceptionally low backgrounds due its front end shielding design and the characteristics of the TS2 source. Further details of the instrument configurations chosen for the simulations will be described in further detail in sections 2 and 3

## 2 Instrument Layout

#### 2.1 SANS2D

SANS2D views the coupled liquid hydrogen moderator on TS2, viewed from the E2 port and operates at 10Hz. This port is in a forward scattering position, which is not ideal for SANS instruments but allowed space for the future addition of a second SANS instrument on E1 which was originally intended to include a focusing option. The original moderator design for which SANS2D was optimised was a coupled, composite, liquid hydrogen, solid methane design with a re-entrant groove which the E1-6 port instruments were intended to view. The current moderator which was installed in 2024 is an 8 cm deep liquid hydrogen moderator viewed through a hole in the beryllium reflector ~85x35 mm in size. The moderator is set back from the beryllium reflector in order to best position it under the neutron target. This moderator provides good long wavelength flux and is a significant improvement on the moderator used between 2011 and 2024 but is still sub-optimal for SANS2D when compared to the original design which had a peak flux at a longer wavelength and significantly better flux at longer wavelengths. Sadly the solid methane design proved to be unstable and would have required unacceptably thick pressure containment walls.

After passing through the collimation in the heavy shutter, a multichannel bender transports and deflects the beam in order to minimise the high energy parasitic neutron and gamma background from the source and feeds the beam though a counter rotating double disk chopper and  $^6$ Li scintillator monitor into a 12m section of heavily shielded interchangeable neutron guide and collimation. 2 m long, evacuated sections of guide may be inserted into the beam path to vary the effective collimation length of the beamline between 2 and 12 m. Between each 2 m section a translatable plate housing a series of different collimation apertures may be used to define the beam size depending on the chosen collimation length. At the end of the collimation a final scraper aperture is position before a second  $^6$ Li scintillator monitor which can be removed from the beam. The final pre-sample collimation section consists of a series of interchangeable B<sub>4</sub>C lined steel collimation tubes onto which the final collimation aperture can be place as close as possible to the sample. The size of this aperture is typically am 8mm or 12mm diameter circle with the initial aperture at the end of the guide section set to 20mm diameter. The sample position is variable and depends on the exact sample environment chosen but is locate at  $\sim$ 19.2 m.

After the sample, the scattered beam enters a large vacuum tank through a 200 mm diameter 7 mm thick c-axis oriented sapphire window. The vacuum tank accommodates two  $\sim 1~\text{m}^2~8$  mm diameter  $^3\text{He}$  tube arrays which can move along the length of the tank providing a a maximum sample to detector distance of 12 m. The instrument simulated in this work places a detector at 12m and the second detector closer to the sample at 5 m with a horizontal offset of 0.86 m. The detector is rotated by 9.4° about its center to reduce parallax errors.

#### 2.2 LoKI

LoKI views the N7 port of the ESS butterfly moderator. As with SANS2D, this port is in a forward scattering position and so the instrument deflects the beam vertically in order to remove direct line of sight of the source. The view is predominantly of the cold coupled moderator face of the overall moderator. The instrument uses a vertical bend to remove direct line of sight of the source which, after a second bender, brings the beam horizontally to the sample position at 23.6 m. Two chopper systems set the wavelength band of the instrument and enable operation at both 14 and 7 Hz. The primary collimation length of the instrument can be varied in steps between 8 ,5 and 3 m using an evacuated, interchangeable guide section located after the second chopper system. Three variable aperture systems are positioned within the collimation section that determine the size of the first SANS aperture. The final collimation section of the beamline prior to the sample is similar to that on SANS2D. The exact position may be varied depending on the sample environment being used so an interchangeable shielded snout section is used to mount the final collimating aperture as close as possible to the sample.

After the sample the scattered beam enters a large vacuum tank which houses a series of detector arrays. A high angle bank consisting of upper and lower detectors locate 1.2 m from the sample and left and right sections located at 1.7 m is fixed is followed by a mid angle bank which has been simulated with the upper and lower sections at 2.95 m from the sample and the left and right sections at 3.3 m. Finally, the low angle bank which can be positioned anywhere between 5 and 10 m from the sample was simulated at a position of 8 m. The actual LoKI detectors consist of complex arrays of boron straw tube detectors that have a significant depth which may lead to parallax errors and will potentially require complex efficiency corrections. This has not been modelled in this work. As with the SANS2D simulations, each detector is considered to be a 100% efficient and is represented by an infinitely thin plane.

#### 3 MonteCarlo Simulations

All Monte Carlo simulations have been carried out using McStas 3.5.1 4, 5, 6, 7, 8 running on an Ubuntu 22.04 windows subsystem for linux run on a windows 11 desktop PC. The SANS2D simulation is based on the model developed by Richard Heenan (ISIS) when the instrument was originally designed. The LoKI model used is based on one kindly provided by Andrew Jackson (ESS).

The original simulation files have been modified to include a new, bespoke detector component developed to output histogram data in radially integrated q. This was done to avoid the need to output data into Mantid 9 or another program in order to produce comparable information. This process would have been very time consuming and results in extremely large data files unnecessarily. The new detector is provided with information about the position of the sample and it's distance from the source. It then calculates the center of the position of the pixel that has been hit relative to the sample in order to allocate intensity to the correct q bin after converting to wavelength from the time-of-flight (TOF) and detector location. These additional steps remove errors that can occur in McStas TOF instrument simulations when using the known wavelength and neutron direction included in the simulation. Using these parameter is incorrect, as it does not reproduce how the actual instrument will function and does not replicate resolution effects that should clearly be present. The detector can be positioned relative to the sample by rotating it around and arm, around it's own local axes and by translating it along and perpendicular to the beam direction. The performance of the detector has been checked by comparing the results generated from simulating a perfect small angle scattering sample with a highly monochromatic source in order to ensure that the expected scattering pattern is reproduced.

For comparison of the simulations of the two instruments two identical samples were used. A flat scattering elastic sample that essentially replicates a perfect vanadium sample used in traditional diffractometer data normalisation and a perfectly monodisperse 100Å radius spherical nanoparticle system included as part of McStas based on the standard scattering calculations included in SASView 10. The settings used for the sample components configured to be exactly the same for both instruments, including the focusing windows which are used to reduce the simulation runtime. A McStas SPLIT call was used to amplify the number of scattering events generated by each neutron hitting the sample by a factor of 1000 for each instrument.

The illuminated sample area was set to 1 cm<sup>2</sup> for both instruments. This is not the setting used for SANS2D in its 12 m configuration where an 8 mm diameter beam is used because of the dimensions of the

sample cells that are typically utilised. Given that LoKI will probably have the same constraint due to the common sample cell geometry it was decided to retain the 1 cm<sup>2</sup> dimension for convenience.

#### 3.1 Intensity Normalisation

For SANS2D the simulation the Commodus\_I3 component was used along with the simulated output from the recent TS2 hydrogen moderator upgrade: Sans2d\_TS2\_HydroMod\_Upgrade2021\_8cmThick.mcstas. For LoKI the setting for the ESS butterfly moderator provided by Andrew Jackson were used. The performance of the moderator in McStas is based on the original 5MW model and so will not directly replicate the performance of the day one science configuration. There is a known disagreement between the ISIS simulated data files and the actual instrument performance which is not accounted for. It is important to consider these limitations during the discussion and results that follow.

In order to normalise the simulation data the detected neutron intensity has been scaled according to the following logic:

#### 3.1.1 SANS2D

The Commodus I3 component outputs intensity in  $ns^{-1}\mu Ahour^{-1}$  so, to reflect the intensity produced by TS2 operating at full power and 10Hz repetition rate this value should be multiplied by a factor of 40.

#### 3.1.2 LoKI

The intensity expected on LoKI at the start of the user program ideally requires a new parametrisation of the McStas ESS moderator component but has been scaled to account for the reduced beam power and energy that will most likely be in use at the start of the user program in 2027. The factors considered and discussed with Andrew Jackson were for an 800 MeV beam energy and 800 kW beam power which is the current strategy. The 800 MeV beam is a reduction from the expected 2 GeV and so calculations have been performed to estimate the impact of this on the observed intensity at each beam port. In addition the day 1 moderator is not the same as the one ultimately envisage for operations which has had a further impact on the expected performance. The factors used for comparison are therefore as follows.

- Factor due to reduced beam energy and moderator configuration differences ×0.36
- Reduced beam power from 2 MW  $\times 800/2000$
- Operation at 7 Hz in order to access the long wavelengths required to reach the lowest q values ×0.5

Overall this results in a reduction factor in the simulated intensity of  $\times 0.072$  compared to the expected performance at 14 Hz with 2 GeV beam energy, 2 MW beam power and with the full specification butterfly moderator. This is a reduction of a factor of  $\sim 14$ .

#### 4 Simulation Results

The run time of simulations were varied to ensure reasonable statistics at the high and low q limits of the data range and so that normalisation of the sphere sample data by the flat scattering sample produced acceptable looking results. The longest simulation run times were approximately 5 minutes. Data is simulated and binned using identical binning in all simulations to enable fair comparisons. Figure 1 shows the integrated intensity from the elastic scattering, flat field sample for the different banks on LoKI and SANS2D. The intensity has been integrated in q and for LoKI the scattering from each of the banks that constitute the high angle bank (HAB) and medium angle bank (MAB) have been summed. For SANS2D the low angle bank (LAB) and high angle bank (HAB) are shown. It is immediately clear that the expected performance gain of LoKI should be significant. This is as a result of both the source characteristics and the additional detector coverage provided by the LoKI detector array. Figure 2 shows the calculated intensity ratios for the LoKI LAB and MAB arrays compared to the SANS2D LAB and HAB array. As expected, there is a significant gain in instrument performance across the whole of the simulated q range, increasing from a factor of ~16

at the lowest q values to 2-3 orders of magnitude at the highest q values. The dip in the ratio at  $\sim 0.09 \text{\AA}^{-1}$  results from the fact that the LoKI HAB shadows the MAB in the instrument as described. This will likely be addressed in the detector commissioning periods and does not significantly affect the results presented here.

Figure 3 shows the simulated data for the monodisperse 100Å diameter sphere sample for each of the detector banks as a function of q. It is immediately clear that the q resolution of SANS2D exceeds that of LoKI at higher q values. This is expected due to the nature of the ESS long-pulse source. However, it is clear that the resolution of LoKI is sufficient to resolve fringes in this perfect sample data at intermediate q values of the order of  $0.1 - 0.2\text{Å}^{-1}$ . It is worth noting that this simulated data is already summing and different wavelengths from different angles and so the resolution function that would be required to fit this data to high precession will be very complex. The wavelength range for SANS2D was set to  $1.75 - 12.5\text{Å}^{-1}$  and  $3.0 - 18.0\text{Å}^{-1}$  for LoKI.

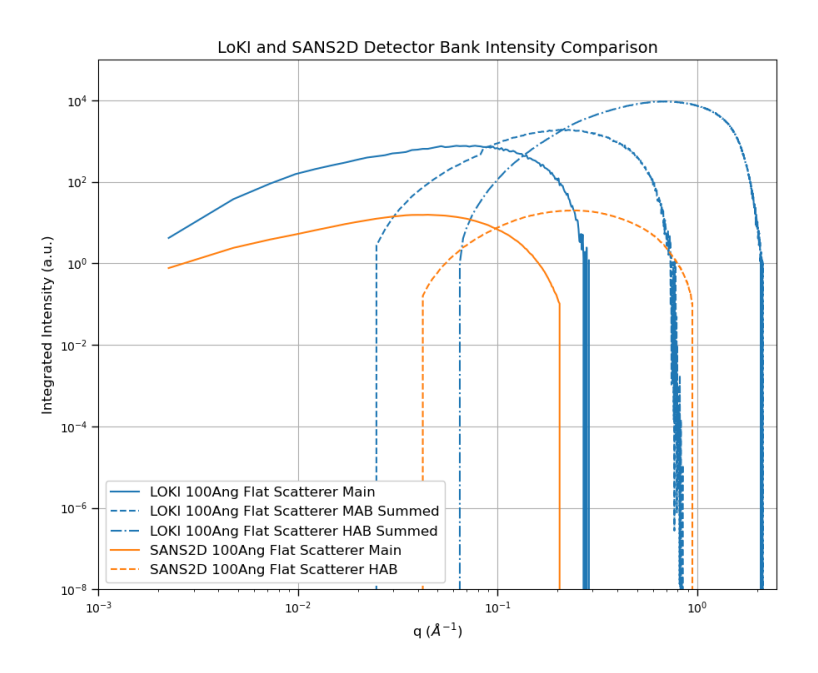


Figure 1: The scattered intensity as a function q for an elastic flat scattering sample for LoKI and SANS2D for each detector bank array.

Figure 3 shows the simulated monodisperse 100Å diameter sphere sample data from the SANS2D LAB and HAB detectors normalised by the flat field sample data along with the same data generated for the LoKI LAB and the upper detector sections of the MAB and HAB arrays. Given the multi-panel geometry of the LoKI detector it was decided this was a farer comparison. The theoretical scattering curve for the sphere sample generated by SASView with no resolution effects is also included for comparison. The SASView curve has been scaled to match the normalised Monte Carlo data. All data were generated with the same binning and q range. The flat field normalisation process highlights the resolution effects produced by the instrument geometry and source characteristics. As was clear in Figure 3 it is straightforward to observe the the high q resolution of LoKI is compromised by the long-pulse nature of the ESS source in the low-angle-bank (Main) detector data. However, it should be noted that the q range at which the resolution smearing is most dramatic is at q values  $> 0.1 \text{Å}^{-1}$ . This will correspond to the region in many SANS experiments where the signal is dominated by incoherent scattering from hydrogen containing samples and so is close to what is generally considered to be the background limited part of the signal. The HAB and MAB detector arrays can be used to recover this resolution. Data illustrating this is shown in figure 5 and figure 6 which compare the flat field normalised data from the 4 banks of the mid and low angle banks to the data from

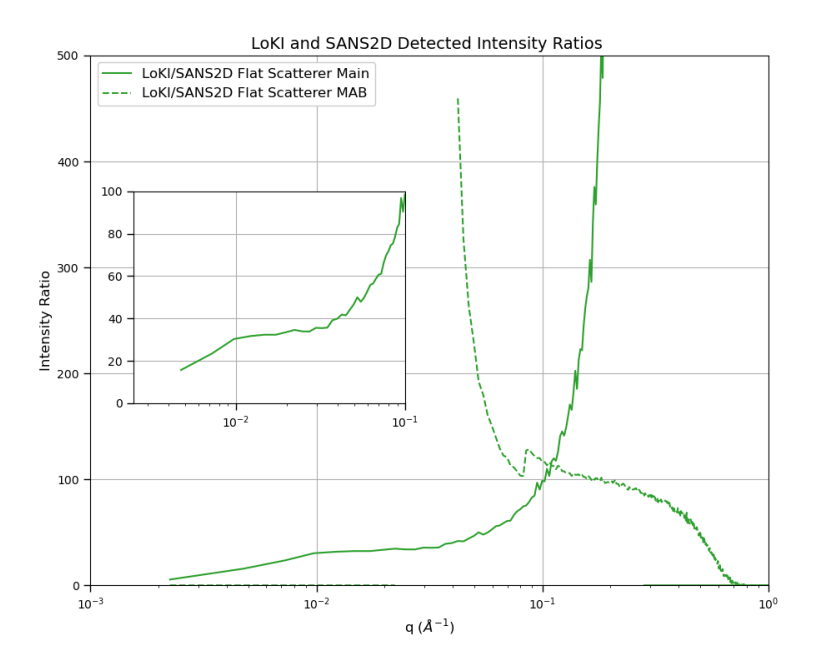


Figure 2: The ratio of scattered intensity as a function q comparing the LoKI Mid Angle Bank and SANS2D and high angle bank. The inset figure provides a zoom in of the lower q region of the curves.

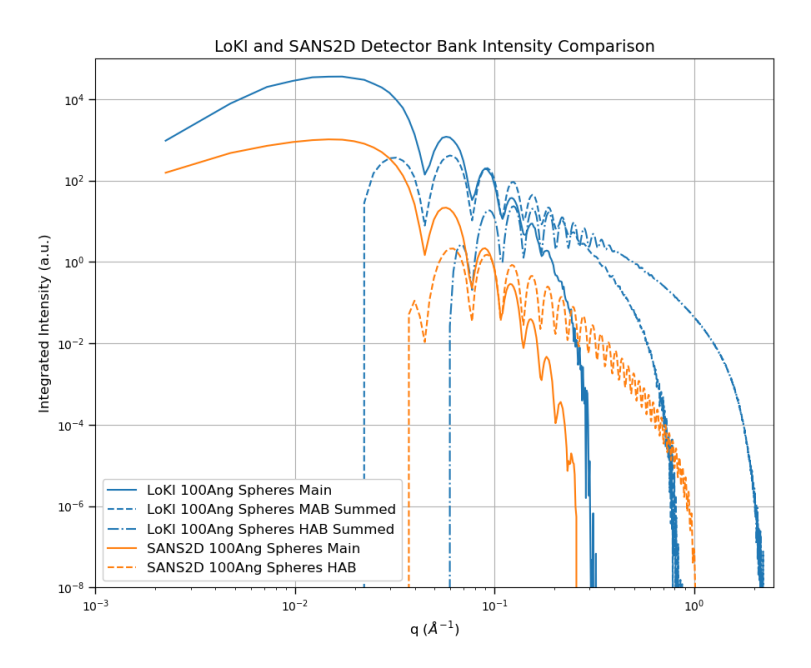


Figure 3: The integrated intensity as a function q for a monodisperse 100Å diameter sphere sample for each detector bank array on LoKI and SANS2D.

the main detector. It is clear that the high angle bank produces higher resolution data more in line with that from SANS2D and that fringes are visible out to q values of  $\sim 0.4\text{\AA}^{-1}$  but beyond this the effects of the long pulse wavelength resolution function damp the data severely. In cases where high angle diffraction studies are needed (>  $0.7\text{Å}^{-1}$ ), choosing another instrument at ESS would be a better choice.

Another feature that is noticeable in figure 5 and figure 6 is that there is an observable difference in the resolution functions of the top-bottom and left-right banks this is to be expected, given the geometry of the instrument this is to be expected but the differences seen here suggest that care should be taken when merging the data from the different detector banks.

Finally, 7 shows that change that should be expected in the pulse shape as a function of wavelength from the ESS source. The changes in the shape of the pulse as a function of wavelength indicate that the effective average time zero of emission for each wavelength should be accounted for in the LoKI data reduction. This has not been accounted for here, the q calculating detector component that has been written accepts a single average T0 offset value that is used to calculate the time of flight of the neutrons. This appears to produce a reasonably robust result but there is a subtle shift in the scattering curve for the monodisperse sphere data shown in figure 4 at low q that could be due to the need to adjust the offset as a function of wavelength. Given the nature of the configuration of the LoKI detector array and the complexity of the data reduction this may well be an effect that is swamped by other more significant systematic problems but it is worth noting as it should be possible to calibrate to remove it.

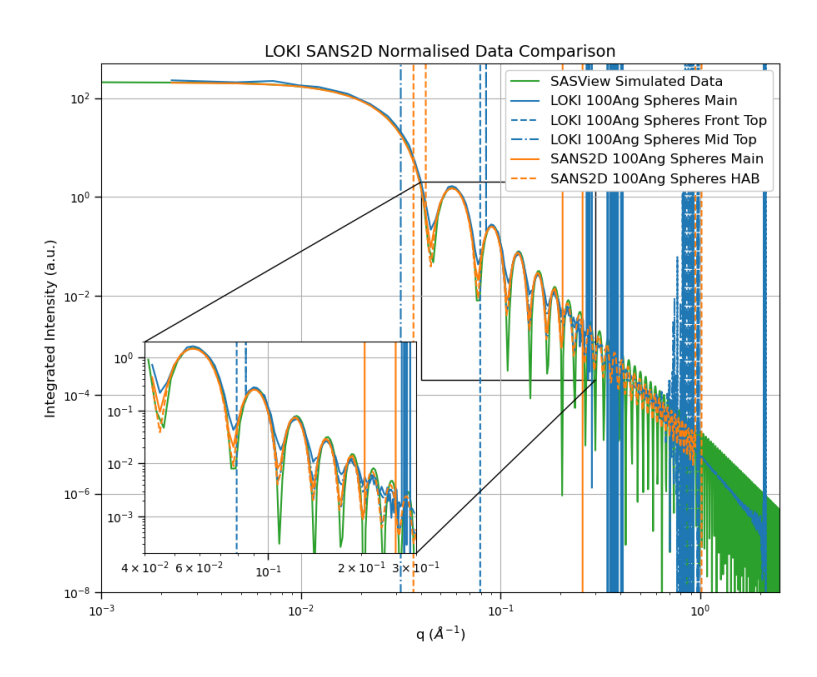


Figure 4: The flat field normalised scattering from a monodisperse 100Å diameter sphere sample shown for the SANS2D LAB and HAB, LoKI HAB-Upper detector, MAB-Upper detector and LAB and compared to the theoretical perfect scattering curve generated by SASView.

#### 5 Conclusions

The performance of LoKI should significantly improve on that of SANS2D if the assumption is made that the inherent background of the instruments are comparable. The detected flux from typical samples predicted for day one user operations should exceed that of SANS2D by a factor of 20 to 30 for the bulk of the typical usable range and by significantly more at higher q assuming that the simulated source intensities used for both instruments are equally uncertain. The backgrounds of SANS measurements of soft matter samples,

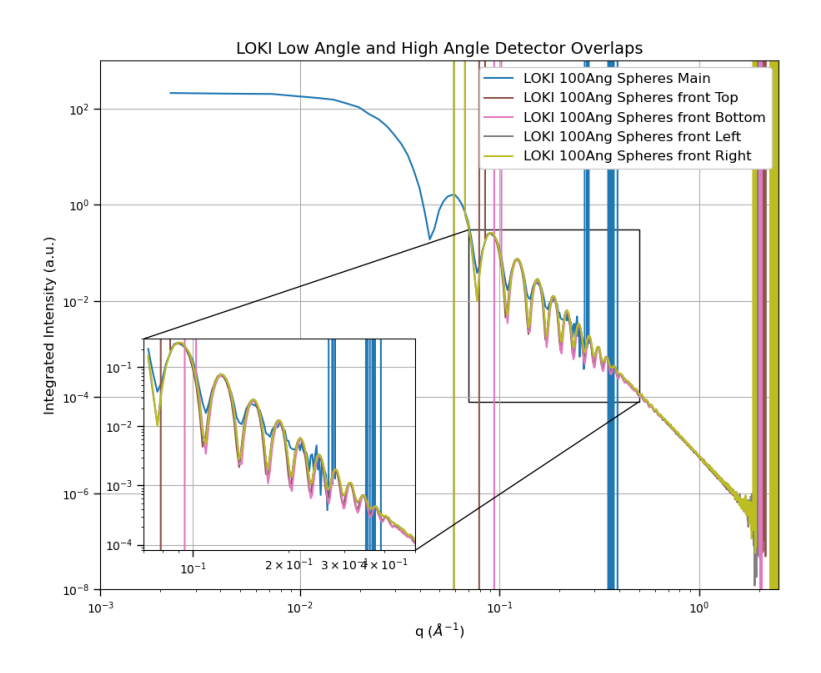


Figure 5: The flat field normalised scattering from a monodisperse 100Å diameter sphere sample shown for the LoKI high-angle-bank arrays compared to the low-angle-bank (main detector)

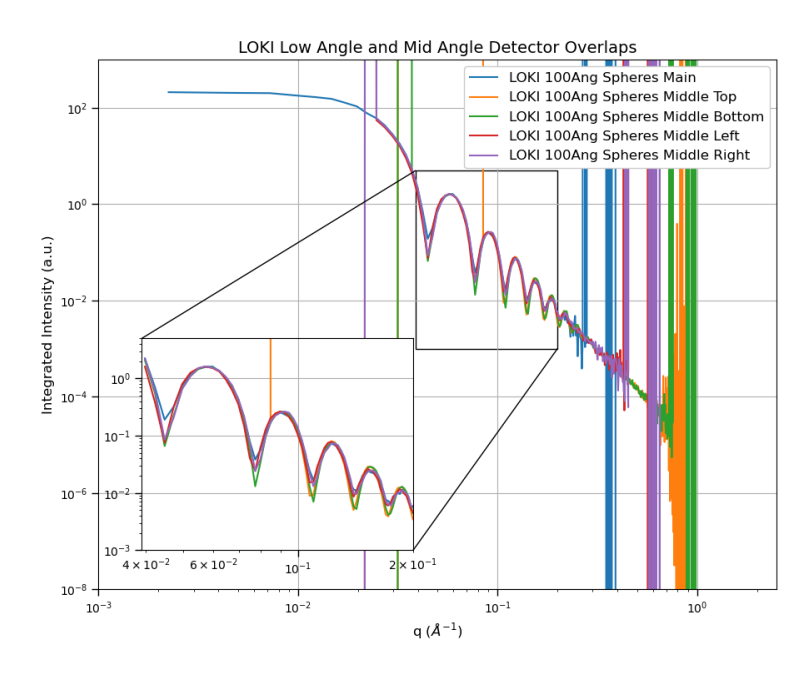


Figure 6: The flat field normalised scattering from a monodisperse  $100\text{\AA}$  diameter sphere sample shown for the LoKI mid-angle-bank arrays compared to the low-angle-bank (main detector)

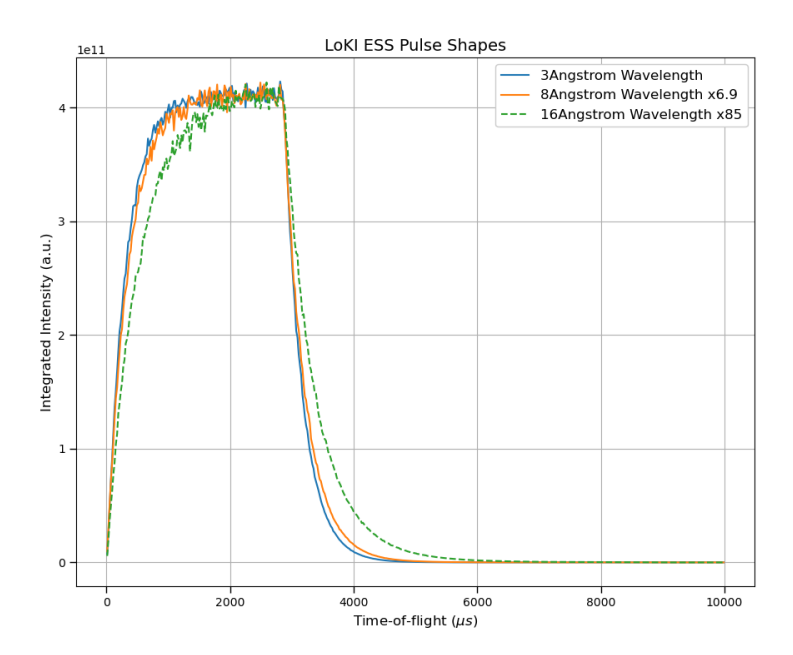


Figure 7: The simulated pulse shapes produced by the ESS moderator as a function of time of flight measure 0.1 mm from the moderator face for 3Å,8Å and 16Å neutrons. The 8Å and 16Å data has been scaled to show the difference in rise time and the length of the tails in the distribution compared to the 3Å data.

which LoKI will typically study, are dominated by sample induced background. This will scale with the flux on sample and so for the low angle bank data in particular there is no reason to suspect that the instrument will not be able to measure at least one order of magnitude quicker than SANS2D for the same size samples. This will enable a significant leap forward in sample throughput but also enable new opportunities as sample sizes can be reduced to areas of a few mm<sup>2</sup> which will be transformative in terms of increasing accessibility by reducing sample cost and also by enabling new sample environment equipment to be developed to study non-equilibrium systems.

A number of questions remain regarding the efficiency, complexity and novelty of the detector array and the complexity of the instrument resolution function. The data reduction will be challenging and is likely to take a significant period of time to thoroughly benchmark and test. The merging of data from different detector banks will require careful consideration and background subtraction from the different detector banks will also need to be looked into in detail. The complexity could potentially introduce additional difficulties into the fitting of data from the instrument and this will, again, likely take a considerable amount of time to benchmark and test.

Beyond day 1, assuming that the ESS gradually ramps up to full beam power and energy (2GeV and 2MW) an additional performance gain over SANS2D of a factor of 7 should be expected while operating in the 8 m low q configuration at 7 Hz. This would be in line with the original expectations of ESS running at 2GeV and 5MW where a gain factor of significantly more than a factor of 100 in performance would be expected.

# 6 Acknowledgements

Thanks to Andrew Jackson (ESS) for providing the LoKI simulation files and providing further input regarding the expected moderator performance for day 1 user program and to Goran Skoro and Rob Bewley (ISIS) for valuable discussions.

### References

- [1] The LoKI instrument webpage at ESS [Online]. Available: https://ess.eu/instruments/loki. [Accessed: September 5, 2025].
- [2] The SKADI instrument webpage at ESS [Online]. Available: https://ess.eu/instruments/skadi. [Accessed: September 5, 2025].
- [3] The SANS2D instrument webpage at ISIS [Online]. Available: https://www.isis.stfc.ac.uk/Pages/sans2d.aspx. [Accessed: September 5, 2025].
- [4] K. Lefmann and K. Nielsen, Neutron News 10, 20, (1999).
- [5] P. Willendrup, E. Farhi and K. Lefmann, Physica B, 350 (2004) 735.
- [6] P. Willendrup, E. Farhi E. Knudsen, U. Filges and K. Lefmann, Journal of Neutron Research, vol. 17, no. 1, pp. 35-43, 2014
- [7] P. Willendrup, and K. Lefmann, Journal of Neutron Research, vol. 22, no. 1, pp. 1-16, 2020
- [8] P. Willendrup, and K. Lefmann, Journal of Neutron Research, vol. 23, no. 1, pp. 7-27, 2021
- [9] Mantid (2025): Manipulation and Analysis Toolkit for Instrument Data.; Mantid Project. http://dx.doi.org/10.5286/SOFTWARE/MANTID/6.9
- [10] The SASView webpage [Online]. Available: http://www.sasview.org/. [Accessed: September 16, 2025].